Impact of Biomass Burning Organic Aerosol Volatility on Smoke Concentrations Downwind of Fires

Demetrios Pagonis,[1,2,3] Vanessa Selimovic,[4,a] Pedro Campuzano-Jost,[1,2] Hongyu Guo,[1,2] Douglas A. Day,[1,2] Melinda K. Schueneman,[1,2] Benjamin A. Nault,[1,2,b] Matthew M. Coggon,[5] Joshua P. DiGangi,[6] Glenn S. Diskin,[6] Edward C. Fortner,[7] Emily M. Gargulinski,[8] Georgios I. Gkatzelis,[2,5,c] Johnathan W. Hair,[6] Scott C. Herndon,[7] Christopher D. Holmes,[9] Joseph M. Katich,[2,5,d] John B. Nowak,[6] Anne E. Perring,[10] Pablo Saide,[11,12] Taylor J. Shingler,[6] Amber J. Soja,[6] Laura H. Thapa,[11] Carsten Warneke,[5] Elizabeth B. Wiggins,[6] Armin Wisthaler,[13,14] Tara I. Yacovitch,[7] Robert J. Yokelson,[4] and Jose L. Jimenez[1,2]

[1]Department of Chemistry, University of Colorado Boulder, Boulder, CO USA
[2]Cooperative Institute for Research in Environmental Sciences (CIRES), University of Colorado, Boulder, CO, USA
[3]Department of Chemistry and Biochemistry, Weber State University, Ogden, Utah, USA
[4]Department of Chemistry, University of Montana, Missoula, MT 59812, USA
[5]NOAA Chemical Sciences Laboratory, Boulder, CO, USA
[6]NASA Langley Research Center, Hampton, VA, USA
[7]Aerodyne Research, Inc., Billerica, MA, USA
[8]National Institute of Aerospace, Hampton, VA, USA
[9]Florida State University Department of Earth, Ocean and Atmospheric Science, Tallahassee, FL, USA
[10]Department of Chemistry, Colgate University, Hamilton, NY, USA
[11]Department of Atmospheric and Oceanic Sciences, University of California, Los Angeles, Los Angeles, CA, USA
[12]Institute of the Environment and Sustainability, University of California, Los Angeles, Los Angeles, CA, USA
[13]Department of Chemistry, University of Oslo, Norway
[14]Institut für Ionenphysik und Angewandte Physik, Universität Innsbruck, Innsbruck, Austria

Now at:
[a]Department of Chemistry, University of Michigan, Ann Arbor, MI 48109
[b]Center for Aerosol and Cloud Chemistry, Aerodyne Research, Inc., Billerica, MA, USA and Department of Environmental Health and Engineering, The Johns Hopkins University, Baltimore, MD, USA
[c]Institute of Energy and Climate Research, IEK-8: Troposphere, Forschungszentrum Jülich GmbH, Jülich, Germany
[d]Ball Aerospace, Boulder, CO, USA

Correspondence: Demetrios Pagonis: demetriospagonis@weber.edu and Jose L. Jimenez: jose.jimenez@colorado.edu

Prepared for *Environmental Science & Technology*

Abstract

Biomass burning particulate matter (BBPM) affects regional air quality and global climate, with impacts expected to continue growing over the coming years. We show that studies of North American fires have a systematic altitude-dependence in measured BBPM normalized excess mixing ratio (NEMR; ΔPM/ΔCO), with airborne and high-altitude studies showing a factor of two higher NEMR than ground-based measurements. We report direct airborne measurements of BBPM volatility that partially explain the difference in BBPM NEMR observed across platforms. We find that when heated to 40-45 ℃ in an airborne thermal denuder, 19% of lofted smoke PM_1 evaporates. Thermal denuder measurements are consistent with evaporation observed when a single smoke plume was sampled across a range of temperatures as the plume descended from 4 km to 2 km altitude. We also demonstrate that chemical aging of smoke and differences in PM emission factors can not fully explain the platform-dependent differences. When the measured PM volatility is applied to output from the HRRR (High Resolution Rapid Refresh)Smoke regional model, we predict lower PM NEMR at the surface compared to the lofted smoke measured by aircraft. These results emphasize the significant role that gas-particle partitioning plays in determining the air quality impacts of wildfire smoke.

Synopsis Statement

Through direct measurements of biomass burning aerosol volatility we explain a significant gap between aerosol concentrations in airborne and ground-based studies.

TOC Art

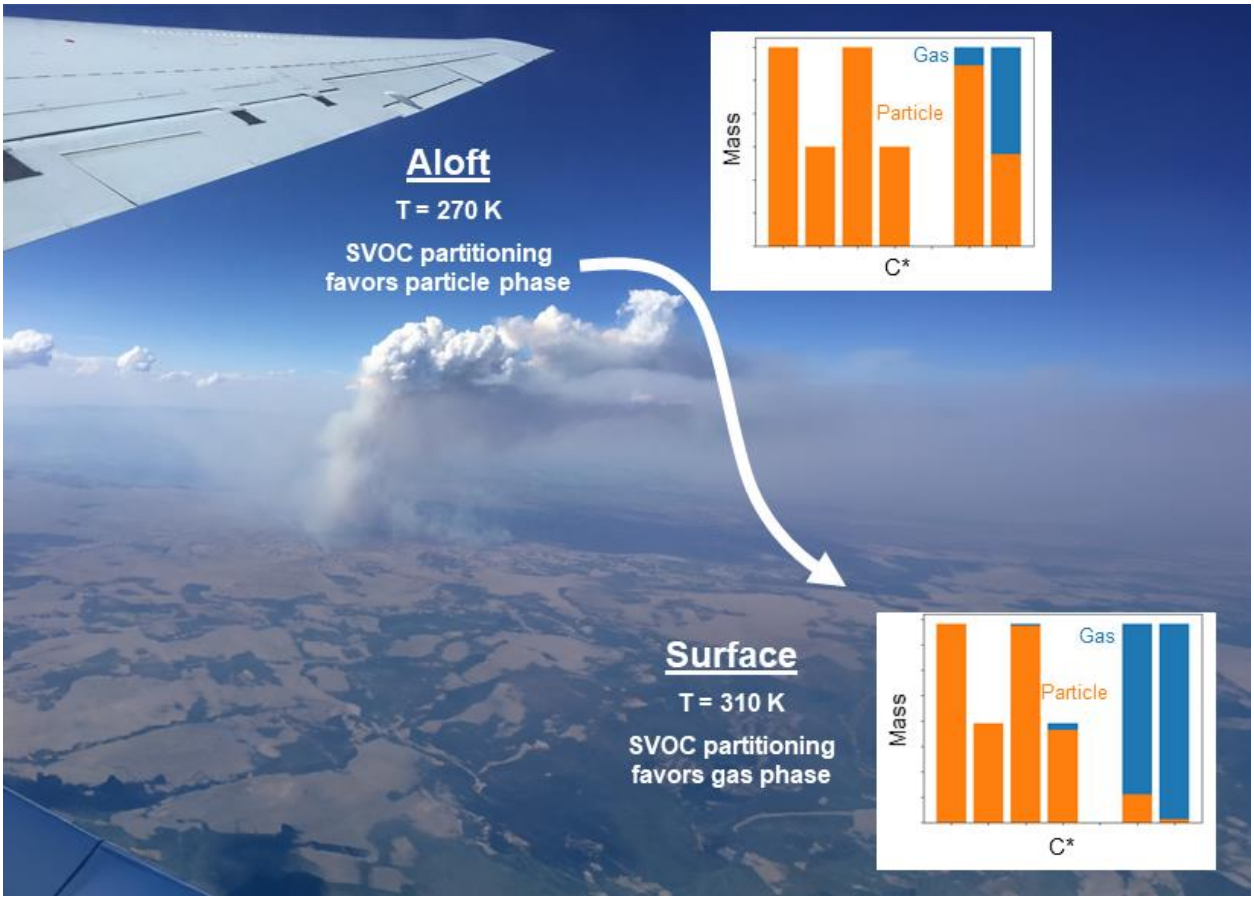
Aloft
T = 270 K
SVOC partitioning
favors particle phase
Gas
Particle
Mass
C*
Surface
T = 310 K
SVOC partitioning
favors gas phase
Gas
Particle
Mass
C*

Introduction

Biomass burning particulate matter (BBPM) emissions cause widespread impacts and dominate the fine particulate matter (PM) burden in regions such as the Western United States.[1,2] The majority of BBPM is organic aerosol (BBOA),[3–6] thus understanding the processes controlling BBOA concentrations is essential to quantify BBPM impacts on health and climate. The health impacts of BBPM are determined by surface burden, while climate impacts are determined by burden across the entire atmosphere. This necessitates study of BBPM at all altitudes. In order to study BBPM in these different parts of the atmosphere, researchers have used several different sampling platforms, each with their own strengths and limitations. Airborne measurements of wildfires are ideal for sampling near-source lofted smoke and studying the first few hours of plume aging, but the contribution of nighttime smoke or unlofted near-surface emissions might be under-estimated or uncharacterized from aircraft.[4,6–8] Fixed surface stations or mobile laboratories downwind of fires are especially well-suited to characterize the overall ground-level impact of regional emissions by collecting data from fires burning at all stages of an entire fire season.[9–12] Ground sites may systematically underrepresent the emissions of more intense fires that are more likely to be lofted into the free troposphere or even the stratosphere[13] Also, determining a smoke age or source measured by these techniques can be especially difficult in situations with multiple mixed sources. Detailed measurements in population centers are less common[9,10,14] and the amount of fire-impacted data collected can depend heavily on chance and the intensity of the fire season. Fixed surface station data may not include specificity on fuels and fire behavior, making it difficult to tease out initial variability and chemical or physical mechanisms contributing to the transformation of smoke. Understanding the differences between smoke sampled by ground and airborne platforms is critical for designing mitigation strategies, planning future wildfire studies,

optimizing satellite retrievals, and determining preferred model inputs for air quality and climate models.[15,16] Efforts to synthesize laboratory, airborne, and ground-based studies of BBOA emissions and evolution have not yielded a clear description of the processes that determine BBOA concentration in different parts of the atmosphere, and the various processes believed to play a role are discussed below.

The literature describing the chemical and physical processes that can impact BBPM normalized excess mixing ratios (NEMR; $\Delta PM/\Delta CO$) is extensive. The key processes emphasized in the literature are: the differences in emissions with fuels combustion state (e.g., flaming vs. smoldering); the differences in the extent of chemical aging experienced during atmospheric transport; and the effects of dilution and temperature on gas-particle partitioning of semivolatile organic compounds.[17–23]

The combustion state of a fire is often characterized with the modified combustion efficiency (MCE), calculated as $\Delta CO_2/(\Delta CO_2+\Delta CO)$, where Δ represents the difference in concentrations between background air and smoke. Many studies have observed a clear relationship between MCE and the emission factor of BBOA (EF_{OA}; $g_{OA}\ kg_{fuel}^{-1}$).[17,24–26] As MCE increases, the conversion of fuel carbon to CO_2 becomes more efficient, and less BBOA is emitted per kg of fuel combusted. Improving our understanding of the relationship between MCE, EF_{OA}, and BBPM NEMR is central to connecting satellite measurements of fire area and/or radiative power (from which mass of fuel combusted can be estimated) to total PM emissions, and thereby PM concentrations downwind of fires. Currently, estimation methods based on measurements of fire radiative power (FRP) can result in good estimates of CO, CO_2, and black carbon emissions, but are more uncertain for estimates of PM, with techniques giving root mean square errors of 46-75% for PM across a recent large-scale field campaign.[27,28]

In a critical review of BBOA aging in laboratory and field studies, Hodshire et al.[20] demonstrate that in laboratory studies chemical aging often produces additional BBOA, while in field studies chemical aging rarely leads to net BBOA production, potentially due to differences in dilution rate and gas-particle partitioning. Results from the WE-CAN aircraft study in the Western US demonstrated that oxidation of measured volatile organic compounds (VOCs) in a smoke plume to form secondary organic aerosol (SOA) could account for just 13% of the SOA formed during aging.[29] The remaining 87% of the SOA was then inferred to be produced by the oxidation of evaporated primary organic aerosol (POA). That study lacked the direct measurements of BBOA volatility aloft that could constrain the extent of POA evaporation downwind of fires.

As is the case for all primary OA sources, some components of primary BBOA are semivolatile and undergo evaporation or condensation as they establish absorptive partitioning equilibrium with the gas phase surrounding each particle. The partitioning equilibrium constant of each compound is determined by the compound's vapor pressure (at a given temperature) and the total concentration of OA.[30,31] Any shifts of the gas-particle partitioning equilibrium will change the BBOA concentration, and will have a direct impact on the observed BBOA NEMR. Dilution and increases in temperature during transport of smoke both lead to net evaporation of BBOA, while decreases in temperature lead to condensation. Thus, the dilution rate of a smoke plume, the background OA concentration, and ambient temperature are expected to be important determinants of the evolution of BBOA NEMR and aerosol optical properties downwind of a fire.[15,32] The volatility distribution of biomass burning emissions has been measured in several ground-based field and laboratory studies, including FLAME III and IV.[21,23] The applicability of these data to real wildfire smoke in different levels of the atmosphere has not been thoroughly assessed.

Previous airborne thermal denuder measurements have heated biomass burning aerosols to hundreds of degrees C in order to separate refractory and non-refractory material.[33] There are presently no published direct measurements of the volatility distribution of organic aerosol from airborne platforms. The volatility of BBOA is not currently accounted for in most operational smoke forecasting models such as HRRR-Smoke and this model has been shown to overpredict smoke concentrations in the Western US.[34]

Here we present results from the FIREX-AQ field study[35] where we conducted airborne thermal denuder measurements that quantified the volatility of bulk BBPM and BBOA, as well as the volatility of key molecular components of BBPM such as levoglucosan and nitrocatechol. These measurements are the first of their kind and serve to constrain the volatility of BBPM. These results are compared to multiple ground and aircraft studies of BBPM in the United States and we compare the variability in BBPM NEMRs observed to the volatility constraints derived from thermal denuder data. We also apply our results to HRRR-Smoke output to estimate the impacts of BBPM volatility on surface smoke concentrations on a regional scale.

Materials and Methods

Field Measurements of BBPM

This study utilizes eleven BBPM datasets from the following campaigns: FIREX-AQ (Fig. S1);[12,35,36] WE-CAN;[37] Missoula, MT; [9,10] BBOP;[17] and SEAC^{4}RS.[24,25] These campaigns cover a variety of fuel types, locations, sampling platforms, and instrumentation. The particulate matter data utilized was either acquired using a high-resolution time-of-flight aerosol mass spectrometer (AMS),[38] an extractive electrospray ionization time-of-flight mass spectrometer (EESI-MS),[36,39] a soot-particle high-resolution time-of-flight aerosol mass spectrometer,[17,40] or an environmental beta-attenuation $PM_{2.5}$ mass monitor.[9,10] The complete list of instrumentation, campaign dates,

platform, fire types sampled, location, number of fires, and analysis details sampled is presented in Table S1 and Section I.

We group these studies into three sets: airborne and high-elevation (>2.5 km above mean sea level) wildland fire studies; airborne agricultural fire studies; and ground-based wildland fire studies (below 1 km above mean sea level). Agricultural fires are separated from the other airborne sampling since they are below 1 km above mean sea level. To compare values from airborne studies with continuous ground-based sampling we reduce all datasets to the fire-day level. For airborne campaigns this means that all transects of a fire from an individual research flight are averaged to a single value; while for ground campaigns smoke impacts are averaged by calendar day. This approach very coarsely averages over diurnal variation in fire behavior in ground studies, and also weights fires of all sizes more equally in airborne studies, since larger fires tend to have longer sampling times (more transects) on a given flight day. The number of fire-days that each campaign was reduced to is presented in Table S1.

Direct Airborne Quantification of BBPM Volatility Distribution

The volatility of BBPM was quantified during FIREX-AQ using airborne thermal denuder (TD) measurements. The TD was a 13 L aluminum cylinder heated to 40-45 °C, followed immediately by a charcoal denuder (ADI; Fort Collins, CO). The TD was a converted potential aerosol mass oxidation flow reactor (PAM OFR)[41,42] operated without ultraviolet lights. The airborne configuration of the PAM OFR on the DC-8 is described in Nault et al,[43] wherein the PAM OFR was used to study aerosol formation potential and aerosol nitrate volatility.[43,44] Concentrations of BBPM components following evaporation in the TD were measured for 15 s every 4 minutes by the University of Colorado AMS[45] and the University of Colorado EESI-

MS.[36,46] Because variations in smoke plume concentrations occurred faster than the residence time of the TD (90 s), a full treatment of the TD residence time distribution is necessary to relate concentrations at the exit of the TD to the unperturbed concentrations in ambient air. The residence time distribution was directly measured with pulse injections of ammonium sulfate and the analyses needed to account for TD residence time and for particle loss within the TD are presented in SI Section II, Figures S3-S6.

Organic Aerosol Emission Factors:

BBOA emission factors (EF_{OA}; g_{OA} kg_{fuel}^{-1}) were calculated using a carbon balance approach,[47] assuming a fuel carbon fraction of 0.5 for forest fires, 0.4 for agricultural fires, and 0.45 for grass fires.[48,49] Species included in the carbon balance were (in decreasing order of abundance): CO_2, CO, the sum of VOCs measured by PTR-ToF-MS, OA, methane, formaldehyde, ethane, and black carbon. Additional details are in the Supplement.

Volatility Basis Set Fitting

The fitted volatility basis set (VBS) used in this work was generated using a brute-force algorithm that utilizes the enthalpy of vaporization parameterization from May et al.[21] In this procedure the bounds and step sizes of the VBS parameters were predefined and the fit quality was assessed for all possible combinations of parameters. A complete description of the parameter space explored is presented in section III of the SI.

Results

Multi-campaign Analysis of BBOA NEMR

Figure 1 presents analysis of BBOA NEMRs from eleven North American studies targeting fire emissions. This analysis shows a systematic altitude / platform dependence in BBOA NEMRs, with the airborne and high-altitude studies measuring NEMRs roughly twice that of ground-based studies. These studies have been carried out by several different research groups using different methods (Table S1 in Supplement) and the platform-dependent trends are robust across those potential sources of variability. One possible explanation for these trends is that the ground-based studies sample air at higher ambient temperatures and therefore semivolatile OA has partially evaporated, decreasing NEMRs. The direct TD measurements of BBPM volatility during FIREX-AQ allow us to explore the extent to which gas-particle partitioning may be driving these trends in NEMRs.

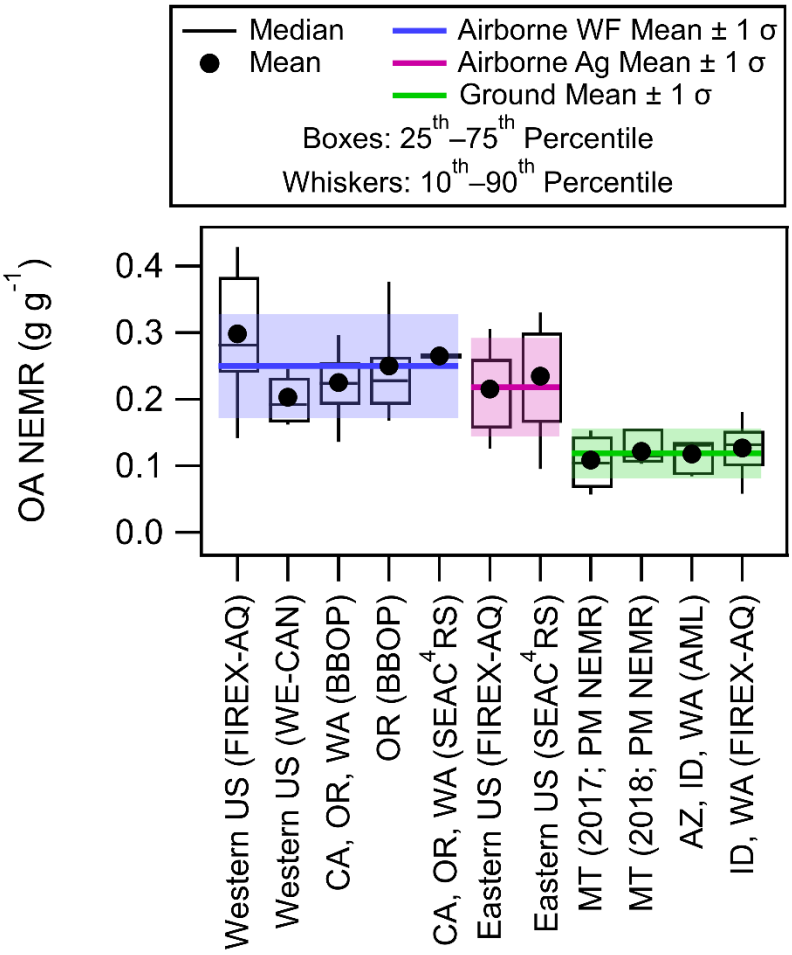

Figure 1. *Comparison of biomass burning particulate matter normalized excess mixing ratio (BBOA NEMR; ΔOA/ΔCO) across multiple campaigns in the United States, demonstrating that airborne and high-altitude studies show OA NEMRs roughly twice as large as those from ground studies. All datasets are averaged to one day to allow comparison across fixed and mobile platforms. Statistical parameters for each campaign are calculated from the one-day data. Shaded regions are the standard deviation of NEMR for each set of campaigns. Note that the two Montana (MT) based ground campaigns are BBPM and not BBOA*

Volatility of BBPM at FIREX-AQ

The experimental design of the TD measurements was to simulate the extent of evaporation that would be expected if lofted smoke were to be transported to lower, warmer altitudes. BBPM loses 19% of its mass when heated from ambient temperatures of 0-5 °C to 40-45 °C. The dependence of MFR on plume concentration and temperature is shown in the Supplement. For comparison to ground studies, the average yearly maximum temperature recorded in Missoula, MT (1990-2020) is 38 °C.[50] Figure 2 presents the results of these measurements for selected components of BBPM. The evaporated mass is primarily BBOA, which comprises over 90% of BBPM mass. We correct for particle wall losses using the non-volatile components sulfate and chloride. Particle chloride at FIREX-AQ is dominated by potassium chloride, which (unlike ammonium chloride) is not volatile at these temperatures.

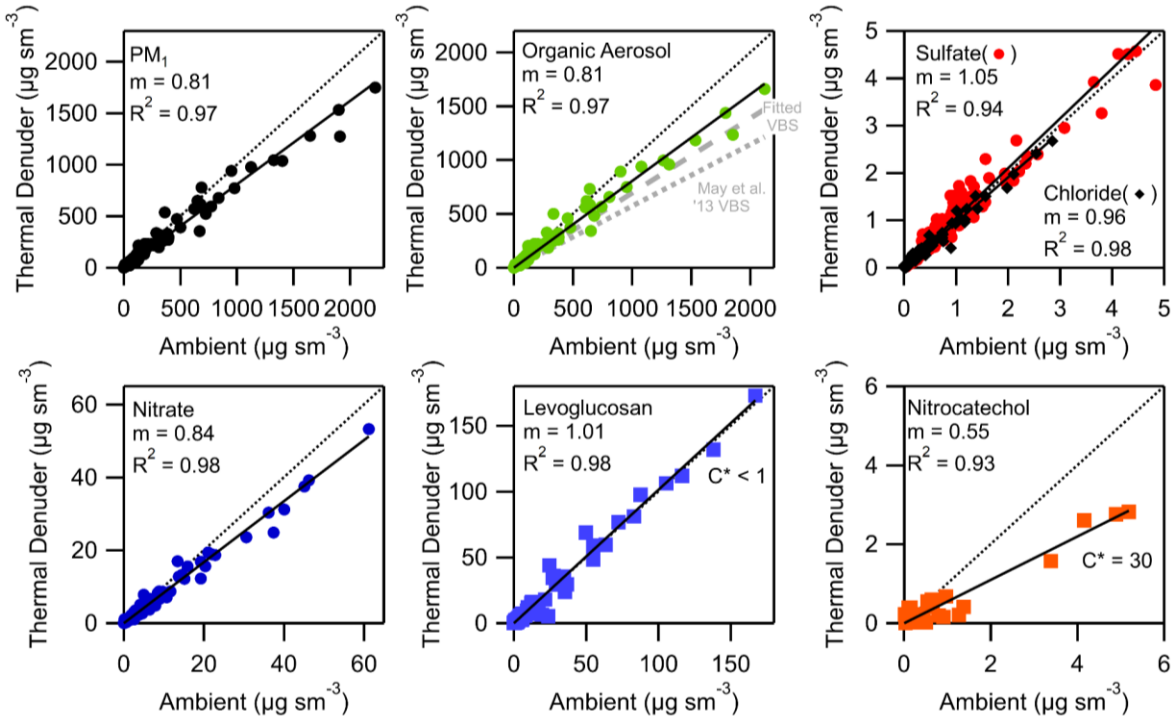

Figure 2. *Results from airborne thermal denuder measurements of biomass burning particulate matter during FIREX-AQ by AMS and EESI-MS. Scatter plots show the concentrations at the output of the thermal denuder (40–45 °C), compared to the input ambient concentrations (0–5 °C). Organic aerosol, nitrate, and nitrocatechol measurably evaporate while aerosol sulfate, chloride, and levoglucosan do not evaporate within measurement uncertainties. The evaporation predicted by this study's fitted VBS is shown in the organic aerosol panel. This figure is presented in log scale in the SI, Figure S2.*

The evaporation of BBOA is modeled using the kinetic TD model of Cappa,[51] which takes a VBS and temperature conditions as inputs and outputs the mass fraction remaining (MFR). We evaluated multiple BBOA VBS from the literature[21,52–55] and also fitted a basis set as part of this work (SI Section III, Figures S7-S9). The fitted basis set is presented in Table S2. Our fitted basis set gives a root mean-squared error (RMSE) of 17%. Of the literature basis sets, the VBS of May et al.[21] performed best (RMSE = 25%), but overpredicted the extent of evaporation under high-OA conditions. Conversely, the VBS derived in this work underpredicts evaporation compared to the May et al. VBS[21] during a natural thermal denuding experiment at concentrations under 100 μg sm^{-3}, as shown in the following section. Comparison of the performance of additional VBS from the literature is presented in the supplement.

The average MFR in the particle phase of levoglucosan and nitrocatechol measured by EESI-MS was 1 and 0.55, respectively (Fig. 2). Prior work has established the attribution of EESI-MS signal to these compounds through the use of offline filter sample analysis.[36] These MFRs correspond to saturation vapor concentrations (C^*_{298}) below 1 μg m^{-3} for levoglucosan and C^*_{298} 30 μg m^{-3} for nitrocatechol. Literature estimates of C^*_{298} for levoglucosan and nitrocatechol are

13 μg m^{-3} [56] and 12-13 μg m^{-3} [57,58] respectively. Literature vapor pressure estimates often vary by an order of magnitude, so these differences are not unexpected.[56] In addition, it is possible that measurement uncertainties, significant non-idealities,[59] or particle-phase reactions of these compounds in smoke particles may impact their gas-particle partitioning. As shown in the following section, the prior measurements of levoglucosan C* are more consistent with the observed evaporation in a natural evaporation experiment, while nitrocatechol C* retrieved in this work performs better than other estimates. Resolving the relationship between the volatility of bulk BBOA and its individual constituents will require significant additional effort that is beyond the scope of this work.

Sheridan Fire Ambient Thermal Denuding Experiment

We further evaluated the volatility of BBPM during FIREX-AQ by measuring smoke emitted from a single fire that was present under a range of ambient temperatures — a natural experiment that allows us to assess the validity of the TD results presented above. Smoke emitted from the Sheridan Fire (Lat. 34.68, Long. -112.89) on August 15th, 2019 was sampled from altitudes of 2-5 km, with the flight track and plume structure shown in Figure 3A, and further analysis of plume rise presented in the Supplement (Section IV, Figure S10). This variability in smoke altitude produced a 17 K temperature gradient in the sampled smoke. The smoke sampled spans a physical age range of 3 h and interpretation of changes in the NEMR is complicated by potential variability in initial fire emissions and chemical aging.

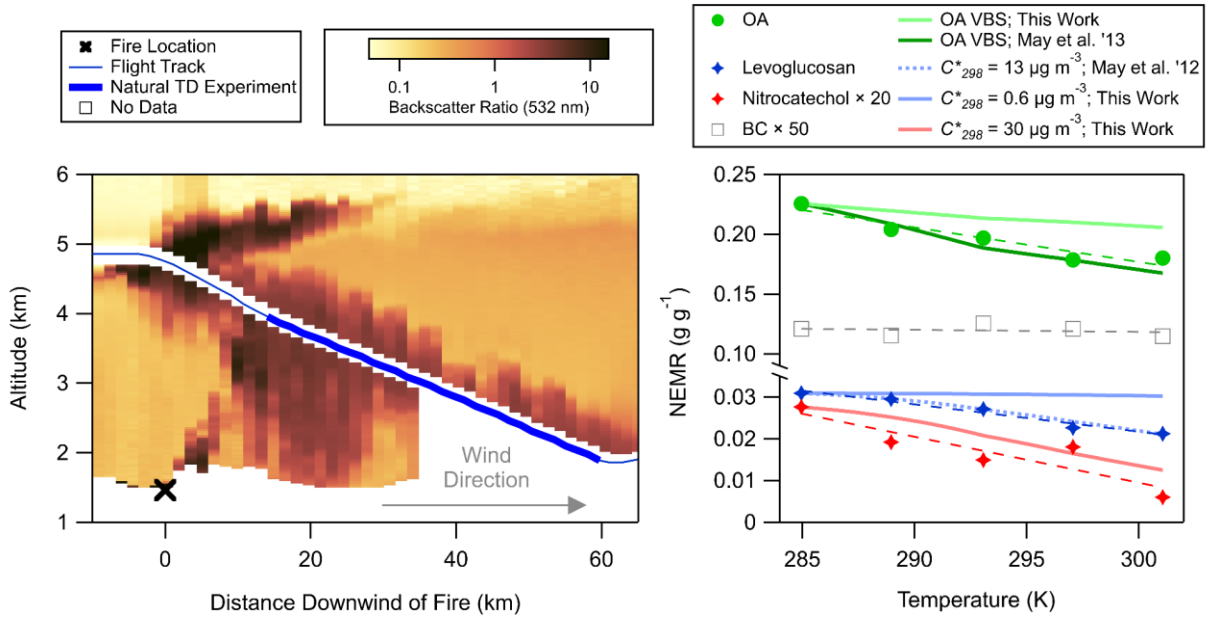

Figure 3. *(A) Sampling of the Sheridan Fire smoke under a range of altitudes (ambient temperatures) during FIREX-AQ (August 16th, 2019 at 01:40–01:46 UTC). The flight track is overlaid on the High Spectral Resolution Lidar backscatter ratio, which is an indicator of BBPM concentration. (B) Changes in OA, BC, aerosol levoglucosan, and aerosol nitrocatechol NEMRs during the plume's descent to lower altitudes (bolded region of panel A). BC NEMR remains constant while OA, levoglucosan, and nitrocatechol NEMRs show decreases consistent with temperature-driven evaporation. Modeled OA evaporation is shown with the fitted VBS from this wok and that of May et al.[21] Modeled levoglucosan and nitrocatechol evaporation are shown using both the C^*_{298} from the literature[21,56] and those derived from the thermal denuder measurements in this work.*

Figure 3B shows no significant change in black carbon NEMR with increasing ambient temperature, suggesting similar initial emissions across different points in the plume, since BC emissions are very sensitive to fire conditions. The VBS fitted to this study's aircraft TD data

underpredicts the extent of BBOA evaporation, with only half of the evaporation accounted for. The May et al. VBS[21] largely reproduces the decrease in OA NEMR. The decrease in levoglucosan NEMR is again underpredicted by our TD fit, but is consistent with previous literature measurements of levoglucosan vapor pressure and ΔH_{vap}.[56] While it is not possible to separate evaporation from the potential impacts of chemical aging and variability in emissions in this case study, the consistency in the OA partitioning trends between Figs. 2 and 3 shows that gas-particle partitioning alone can plausibly explain the variability in OA NEMR observed at the Sheridan fire.

OA Emission Factors

In the following sections, we examine the campaign-wide relationship between OA NEMR, OA emission factor, MCE, and smoke age from the FIREX-AQ dataset. MCE was calculated from the slope of a York regression of CO and CO_2 concentrations. We find that the effects of MCE and age are significantly smaller than the large shifts in OA NEMR resulting from the semivolatile nature of BBOA. As shown in Fig. 4, EF_{OA} exhibits a linear dependence with MCE. This relationship has been observed in previous BBOA airborne campaigns.[17,24–26] These studies did not all show the same trend between EF_{OA} and MCE, but they mostly lie within the variability of the larger FIREX-AQ dataset. This result indicates that prior apparent disagreement among smaller campaigns could be partially due to variability in emissions, given the smaller number of fires sampled in those studies.

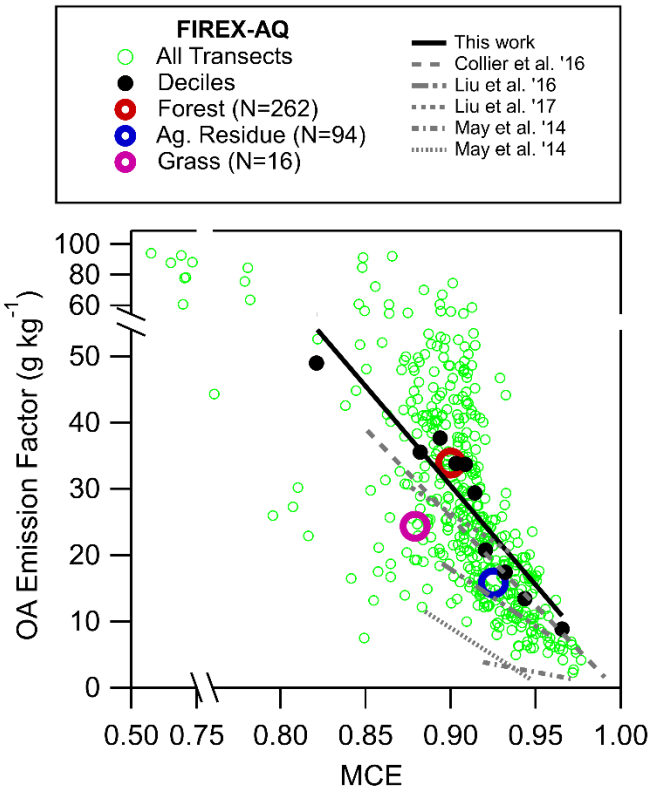

Figure 4. *MCE dependence of OA emission factors for all plume transects (N=489) during FIREX-AQ. Fuel-specific emission factor averages are overlaid. Fuel-specific fits showing a consistent relationship between emission factor and MCE across fuels are presented in Fig S11. The variability of the FIREX-AQ data spans most of the range of observations from previously published airborne studies.*

Average emission factors for the three primary fuel types in FIREX-AQ (forest, total transects (N) = 307; agricultural residue, N = 117; and grass, N = 21) are shown in Fig. 4. EF_{OA} for each fuel type follows a similar MCE dependence (Fig. S11, indicating that MCE-driven variability in EF_{OA} is more significant than fuel-driven variability in EF_{OA}.

Critically, the linear dependence of OA emission factors with MCE cannot explain the difference between ground and airborne studies shown in Fig. 1. This is because a species whose

emission factor varies linearly with MCE will show no correlation between NEMR and MCE (Fig. 5A), because the emission factor of CO is also varying (almost) linearly with MCE in the same way (MCE = $\Delta CO_2/(\Delta CO_2+\Delta CO)$). Quantification of MCE and fuel loading are crucial to producing accurate estimates of the total quantity of PM emitted by a fire, but this result shows that MCE- and fuel-driven differences in BBPM emission fluxes will not cause the platform-dependent variability in BBPM NEMR shown in Fig. 1. Differences in MCE can explain the differences in BC NEMR observed across campaigns (Fig. S12), because BC emissions do not vary linearly with MCE.[26]

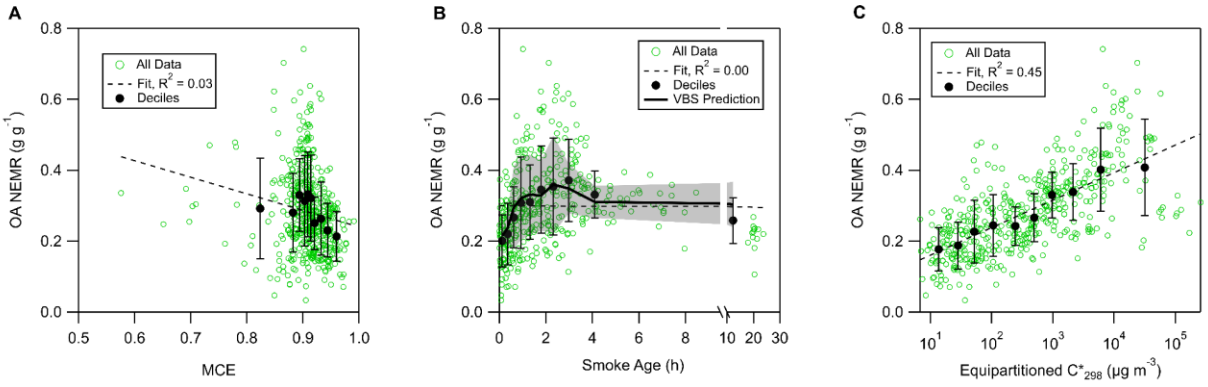

Figure 5. *The OA NEMR measured during FIREX-AQ, as a function of fire MCE (A), physical smoke age (B), and the volatility of compounds expected to be equally partitioned between the gas and particle phases (C). The trend in (C) shows that gas-particle partitioning is a major driver of OA NEMR in the FIREX-AQ dataset. Error bars are standard deviations within each decile, and the shading in (B) is the standard deviation of each decile for the VBS prediction.*

Aging of Biomass Burning Organic Aerosol:

The relationship between OA NEMR and physical smoke age in the airborne FIREX-AQ dataset is shown in Fig. 5B. Without accounting for other factors, there is an apparent trend of increasing OA NEMR within the first 3 hours of aging, from 0.2 g g^{-1} to 0.3 g g^{-1}, but there is a strong correlation in the FIREX-AQ dataset between smoke age and air temperature, with fresh smoke being roughly 25 K hotter than smoke that is 4 h old (Fig. S12). This difference in temperature has the potential to produce significantly lower OA NEMRs for fresh smoke, which is what we observe in Fig. 5B. To separate the effects of gas-particle partitioning and SVOC evaporation from those of chemical aging, we can use the VBS derived in this work to explore the anticipated trends in OA NEMR at the plume temperatures and concentrations sampled at FIREX-AQ. First, we derive the MCE dependence of the SVOC emission factor using the VBS fitted to the TD data above (SI Section V, Figure S14). Then we use the plume MCE and summed carbon concentration to calculate the total SVOC concentration for each plume transect (C_{SVOC} (μg sm^{-3}) = EF_{SVOC} (g kg $fuel^{-1}$) × C_{Carbon} (μg sm^{-3}) / $\%C_{Fuel}$). Finally we solve the gas-particle partitioning equilibrium at the plume air temperature and pressure. The OA NEMR is then calculated for all plume transects, averaged into deciles, and compared to observed OA NEMR deciles in Fig.5A. The majority of the observed increase in OA NEMR with smoke age is accounted for by the fact that plumes sampled at > 3 h age are both colder and had a higher OA concentration than plumes that were only sampled at ages < 3 h. Fire and plume size play a clear role in this effect: only the largest fires produced plumes that were sufficiently coherent and concentrated to be sampled across many hours of aging. Rates of chemical aging can vary widely from one smoke plume to another, and so we also conducted an identical analysis using the furan:maleic anhydride photochemical clock[60] in place of physical age. Our conclusions for chemical age are the same as

those seen for physical age (Fig S15). From this, we conclude that the aging of BBOA only has a minor impact on BBPM NEMR compared to gas-particle partitioning. This result is consistent with the data of Palm et al.,[29] but we ascribe a fundamentally different mechanism to the trend. Palm et al.[29] attributes all increases in BBPM NEMR to formation of SOA and since only 13% percent of the shift in NEMR is attributable to SOA from VOC precursors, it is assumed that the remaining 87% of the increase in OA NEMR observed during WE-CAN is due to the evaporation and subsequent oxidation of POA. Our data suggests that in fact these trends are wholly explainable by the initial volatility distributions of BBOA. While there is certainly aging of evaporated POA occurring as smoke travels (trends in O:C ratio of BBOA presented in Fig. S16),[20,22] our results indicate that chemical aging was not producing a noticeable shift in the volatility distribution of the organic compounds. Accordingly, models which aim to capture BBPM concentrations (as opposed to composition) might choose to prioritize parameterizations of BBPM volatility and emission factors over descriptions of chemical aging.

Quantifying Gas-Particle Partitioning

The extent of gas-particle partitioning for a smoke plume depends on the plume BBOA concentration and air temperature. In the FIREX-AQ dataset temperature and plume concentration are both highly variable and so it is desirable to express the state of gas-particle equilibrium with a single parameter. We do this by calculating the volatility (C^*_{298}) of compounds that are expected to be evenly partitioned between the gas and particle phase. This calculation involves taking the equipartitioned C* at the temperature of the plume (which is equal to the OA concentration) and calculating the vapor pressure at 298 K according to the ΔH_{vap} parameterization used in this work.[21] This parameter (equipartitioned C^*_{298}) describes the extent to which the particle phase is favored

in the gas-particle partitioning equilibrium and gives a better correlation with OA NEMR than either plume OA concentration or temperature independently (Fig. S17). A higher equipartitioned C^*_{298} indicates that the particle phase is heavily favored (since higher-volatility compounds are found in the particle phase), while a very low equipartitioned C^*_{298} indicates that only the lowest-volatility compounds are found in the particle phase. As shown in Fig. 5C, the equipartitioned C^*_{298} describes the variability in OA NEMR during FIREX-AQ better than age or MCE. This result supports the assumption underlying this work that there is a consistent SVOC:CO emission ratio from fires in the United States (Fig S14). Because of this conclusion, we expect that differences in plume concentration and temperature across multiple campaigns contribute to the platform-dependent BBPM NEMR difference shown for North American campaigns above.

Applying VBS to High-Resolution Rapid Refresh (HRRR)-Smoke

To assess the impacts of gas-particle partitioning on smoke concentrations on a regional scale and to determine if the BBOA volatility constrained in this study can explain the differences in BBPM NEMR shown in Fig. 1, we apply the FIREX-AQ VBS and emission factors to output from the High Resolution Rapid Refresh Smoke (HRRR-Smoke) model from a single point in time from summer 2018,[61] where bins are assumed to be smoke-impacted if they have over 1 $\mu g\ m^{-3}$ of BBPM and bins below this threshold are excluded. HRRR-Smoke represents PM as a chemically inert tracer, which allows us to scale HRRR-Smoke surface PM concentration to a VBS concentration using the ratio of the average FIREX-AQ emission factors for PM and SVOC ($C_{SVOC} = C_{PM,HRRR} \times EF_{SVOC} / EF_{PM}$). Gas-particle partitioning of the SVOC is then solved for each surface-level grid cell to arrive at PM concentrations. In effect, this analysis lets us approximately translate from the chemically-inert PM tracer in HRRR-Smoke to a VBS representation of gas-

particle partitioning. These results are shown for HRRR-Smoke output from August 3, 2018 in Fig. 6. Across the United States, this model exercise predicts that gas-particle partitioning produces a median reduction in surface smoke concentrations of 31%, and there is a clear relationship between the concentration of surface smoke in HRRR output and the shifts in gas-particle partitioning predicted by the VBS.

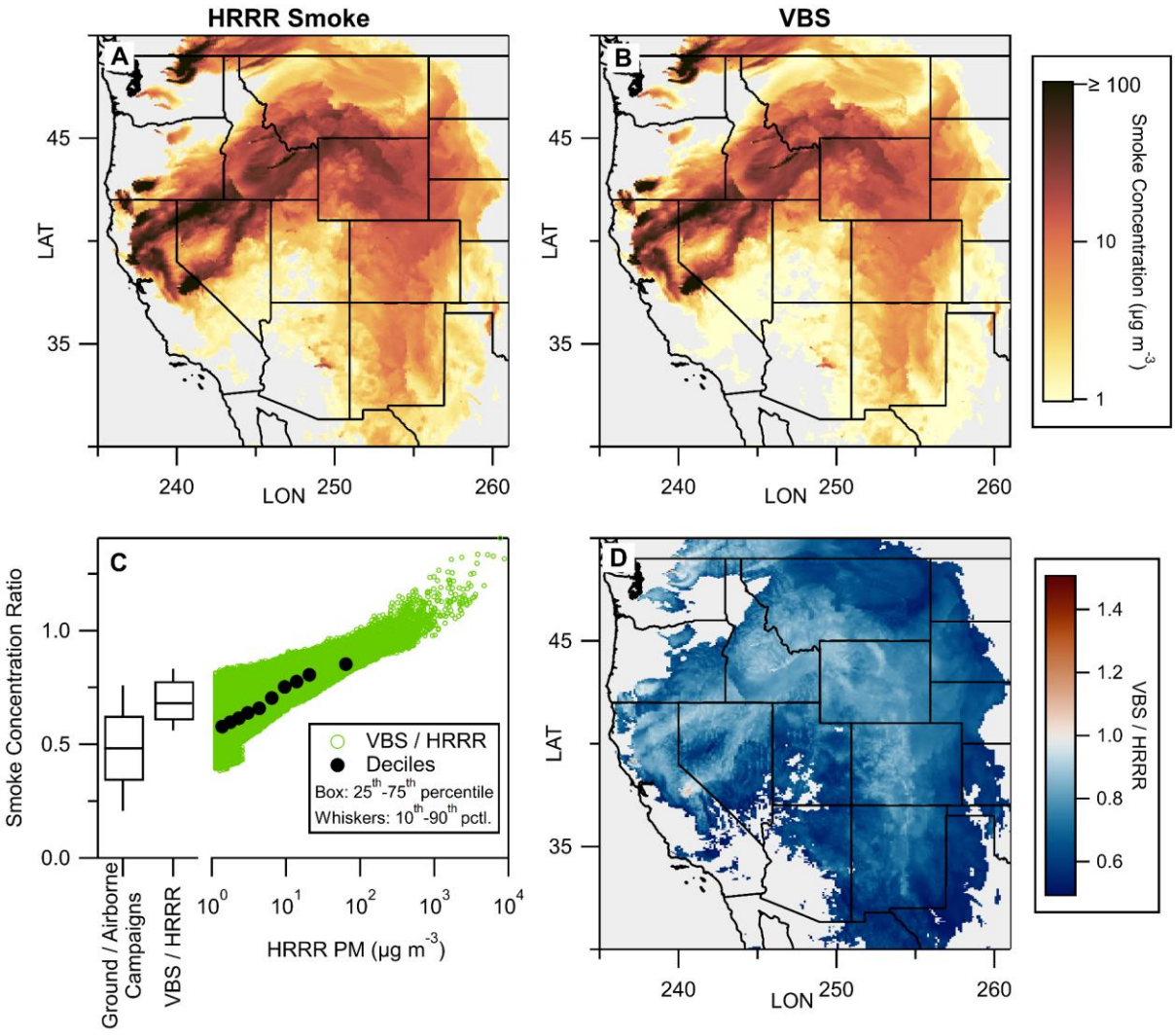

Figure 6. *Application of this work's SVOC emission ratios to the HRRR Smoke model output for surface smoke concentrations from August 3, 2018 (A and B). Accounting for evaporation of BBPM at surface temperatures reduces surface concentrations by 31%, approximately two thirds*

of the difference observed between ground and airborne campaigns in the United States (C and D).

Accordingly, the results shown in Fig. 6C explain over half of the platform-dependent trends seen in our compilation of wildfire studies in the United States (Fig. 1). Airborne and high-altitude studies are at higher concentrations and lower temperatures than ground-based studies and semivolatile compounds favor the particle phase, increasing the OA NEMR (Fig. S18). In warmer and more dilute ground-based studies, semivolatile compounds favor the gas phase, leading to lower OA NEMRs. We hypothesize that the remaining difference between ground-based and airborne studies may be due to factors such as dry deposition,[62] in addition to smaller impacts of aging chemistry and differences in emissions.

These measurements show that volatility basis sets measured through laboratory studies of smoke emissions are directly applicable to ambient smoke in the troposphere. Similarly, laboratory studies of the volatility of individual components of BBPM are consistent with evaporation observed in the field, within the typical order-of-magnitude uncertainty in SVOC vapor pressure. We show that BBPM emission factors depend more on MCE than fuel identity; and that chemical aging has a minor effect on BBPM NEMR up to 20 hours downwind of fires. These results indicate that accurate characterization of gas-particle partitioning, fuel loading, and combustion state have the greatest potential to improve BBPM forecasts. Further study of BBOA volatility and altitude-dependent partitioning would advance our understanding of how evaporating BBOA impacts air quality at the surface.

Acknowledgements

We thank the crews, pilots, and support staff from all the field campaigns included for making these measurements possible. The CU HR-AMS team was funded by NASA grants 80NSSC18K0630, 80NSSC19K0124 and 80NSSC21K1451. Work by DP at Weber State University was funded by NASA grant 80NSSC21K1451. VS and RY were supported by the NSF grant AGS-1748266 and NOAA-CPO grant NA16OAR4310100. The WE-CAN measurements herein were supported by the NOAA OAR Climate Program Office Award Number NA17OAR4310010. We acknowledge the work of many additional scientists for the generation and analysis of the data used in this work. This includes, but is not limited to: Eben Cross, Conner Daube, Christoph Dyroff, Delphine Farmer, Andy Freedman, Alan Fried, Lauren Garofalo, Hannah Halliday, Anne Handschy, Thomas Hanisco, Jordan Krechmer, Matson Pothier, J. Rob Roscioli, Joshua Schwarz, and Glenn Wolfe.

Supporting Information

Campaign summary information; calculation of normalized excess mixing ratios; thermal denuder analysis; evaluation of literature and fitting of volatility basis sets; Sheridan fire plume dynamics; calculation of emission factors; correlation of FIREX-AQ smoke age with temperature.

Data Availability

FIREX-AQ data is available at the NASA LARC archive (10.5067/SUBORBITAL/FIREXAQ2019/DATA001). WE-CAN data is available through the NCAR Earth Observing Laboratory (https://data.eol.ucar.edu/master_lists/generated/we-can/).

References

(1) Jaffe, D. A.; O'Neill, S. M.; Larkin, N. K.; Holder, A. L.; Peterson, D. L.; Halofsky, J. E.; Rappold, A. G. Wildfire and Prescribed Burning Impacts on Air Quality in the United States. *J. Air Waste Manag. Assoc.* **2020**, *70* (6), 583–615.

(2) McClure, C. D.; Jaffe, D. A. US Particulate Matter Air Quality Improves except in Wildfire-Prone Areas. *Proc. Natl. Acad. Sci. U. S. A.* **2018**, *115* (31), 7901–7906.

(3) Andreae, M. O. Emission of Trace Gases and Aerosols from Biomass Burning – an Updated Assessment. *Atmos. Chem. Phys.* **2019**, *19* (13), 8523–8546.

(4) Akagi, S. K.; Yokelson, R. J.; Wiedinmyer, C.; Alvarado, M. J.; Reid, J. S.; Karl, T.; Crounse, J. D.; Wennberg, P. O. Emission Factors for Open and Domestic Biomass Burning for Use in Atmospheric Models. *Atmos. Chem. Phys.* **2011**, *11*, 4039–4072.

(5) Stockwell, C. E.; Bela, M. M.; Coggon, M. M.; Gkatzelis, G. I.; Wiggins, E.; Gargulinski, E. M.; Shingler, T.; Fenn, M.; Griffin, D.; Holmes, C. D.; Ye, X.; Saide, P. E.; Bourgeois, I.; Peischl, J.; Womack, C. C.; Washenfelder, R. A.; Veres, P. R.; Neuman, J. A.; Gilman, J. B.; Lamplugh, A.; Schwantes, R. H.; McKeen, S. A.; Wisthaler, A.; Piel, F.; Guo, H.; Campuzano-Jost, P.; Jimenez, J. L.; Fried, A.; Hanisco, T. F.; Huey, L. G.; Perring, A.; Katich, J. M.; Diskin, G. S.; Nowak, J. B.; Bui, T. P.; Halliday, H. S.; DiGangi, J. P.; Pereira, G.; James, E. P.; Ahmadov, R.; McLinden, C. A.; Soja, A. J.; Moore, R. H.; Hair, J. W.; Warneke, C. Airborne Emission Rate Measurements Validate Remote Sensing Observations and Emission Inventories of Western U.S. Wildfires. *Environ. Sci. Technol.* **2022**. https://doi.org/10.1021/acs.est.1c07121.

(6) Yokelson, R. J.; Crounse, J. D.; DeCarlo, P. F.; Karl, T.; Urbanski, S.; E. Atlas; Campos, T.; Shinozuka, Y.; Kapustin, V.; Clarke, A. D.; Weinheimer, A.; Knapp, D. J.; Montzka, D. D.; Holloway, J.; Weibring, P.; Flocke, F.; Zheng, W.; Toohey, D.; Wennberg, P. O.; Wiedinmyer, C.; Mauldin, L.; Fried, A.; Richter, D.; Walega, J.; Jimenez, J. L.; Adachi, K.; Buseck, P. R.; Hall, S. R.; Shetter, R. Emissions from Biomass Burning in the Yucatan. *Atmos. Chem. Phys.* **2009**, *9* (15), 5785–5812.

(7) Yokelson, R. J.; Christian, T. J.; Karl, T. G.; Guenther, A. The Tropical Forest and Fire Emissions Experiment: Laboratory Fire Measurements and Synthesis of Campaign Data. *Atmos. Chem. Phys.* **2008**, *8* (13), 3509–3527.

(8) Akagi, S. K.; Burling, I. R.; Mendoza, A.; Johnson, T. J.; Cameron, M.; Griffith, D. W. T.; Paton-Walsh, C.; Weise, D. R.; Reardon, J.; Yokelson, R. J. Field Measurements of Trace Gases Emitted by Prescribed Fires in Southeastern US Pine Forests Using an Open-Path FTIR System. *Atmos. Chem. Phys.* **2014**, *14* (1), 199–215.

(9) Selimovic, V.; Yokelson, R. J.; McMeeking, G. R.; Coefield, S. Aerosol Mass and Optical Properties, Smoke Influence on O 3 , and High NO 3 Production Rates in a Western US City Impacted by Wildfires. *J. Geophys. Res. D: Atmos.* **2020**. https://doi.org/10.1029/2020JD032791.

(10) Selimovic, V.; Yokelson, R. J.; McMeeking, G. R.; Coefield, S. In Situ Measurements of Trace Gases, PM, and Aerosol Optical Properties during the 2017 NW US Wildfire Smoke Event. *Atmos. Chem. Phys.* **2019**, *19* (6), 3905–3926.

(11) Wiggins, E. B.; Andrews, A.; Sweeney, C.; Miller, J. B.; Miller, C. E.; Veraverbeke, S.; Commane, R.; Wofsy, S.; Henderson, J. M.; Randerson, J. T. Boreal Forest Fire CO and CH_4 Emission Factors Derived from Tower Observations in Alaska during the Extreme Fire Season of 2015. *Atmos. Chem. Phys.* **2021**, *21* (11), 8557–8574.

(12) Majluf, F. Y.; Krechmer, J. E.; Daube, C.; Knighton, W. B.; Dyroff, C.; Lambe, A. T.; Fortner, E. C.; Yacovitch, T. I.; Roscioli, J. R.; Herndon, S. C.; Worsnop, D. R.; Canagaratna, M. R. Mobile Near-Field Measurements of Biomass Burning Volatile Organic Compounds: Emission Ratios and

Factor Analysis. *Environ. Sci. Technol. Lett.* **2022**, *9* (5), 383–390.
(13) Peterson, D. A.; Thapa, L. H.; Saide, P. E.; Soja, A. J.; Gargulinski, E. M.; Hyer, E. J.; Weinzierl, B.; Dollner, M.; Schöberl, M.; Papin, P. P.; Kondragunta, S.; Camacho, C. P.; Ichoku, C.; Moore, R. H.; Hair, J. W.; Crawford, J. H.; Dennison, P. E.; Kalashnikova, O. V.; Bennese, C. E.; Bui, T. P.; DiGangi, J. P.; Diskin, G. S.; Fenn, M. A.; Halliday, H. S.; Jimenez, J.; Nowak, J. B.; Robinson, C.; Sanchez, K.; Shingler, T. J.; Thornhill, L.; Wiggins, E. B.; Winstead, E.; Xu, C. Measurements from inside a Thunderstorm Driven by Wildfire: The 2019 FIREX-AQ Field Experiment. *Bull. Am. Meteorol. Soc.* **2022**, *103* (9), E2140–E2167.
(14) Lill, E.; Lindaas, J.; Juncosa Calahorrano, J. F.; Campos, T.; Flocke, F.; Apel, E. C.; Hornbrook, R. S.; Hills, A.; Jarnot, A.; Blake, N.; Permar, W.; Hu, L.; Weinheimer, A.; Tyndall, G.; Montzka, D. D. e.; Hall, S. R.; Ullmann, K.; Thornton, J.; Palm, B. B.; Peng, Q.; Pollack, I.; Fischer, E. V. Wildfire-Driven Changes in the Abundance of Gas-Phase Pollutants in the City of Boise, ID during Summer 2018. *Atmos. Pollut. Res.* **2022**, *13* (1), 101269.
(15) Reid, J. S.; Koppmann, R.; Eck, T. F.; Eleuterio, D. P. A Review of Biomass Burning Emissions Part II: Intensive Physical Properties of Biomass Burning Particles. **2005**.
(16) Reid, J. S.; Hyer, E. J.; Prins, E. M.; Westphal, D. L.; Zhang, J.; Wang, J.; Christopher, S. A.; Curtis, C. A.; Schmidt, C. C.; Eleuterio, D. P.; Richardson, K. A.; Hoffman, J. P. Global Monitoring and Forecasting of Biomass-Burning Smoke: Description of and Lessons From the Fire Locating and Modeling of Burning Emissions (FLAMBE) Program. *IEEE Journal of Selected Topics in Applied Earth Observations and Remote Sensing* **2009**, *2* (3), 144–162.
(17) Collier, S.; Zhou, S.; Onasch, T. B.; Jaffe, D. A.; Kleinman, L.; Sedlacek, A. J., 3rd; Briggs, N. L.; Hee, J.; Fortner, E.; Shilling, J. E.; Worsnop, D.; Yokelson, R. J.; Parworth, C.; Ge, X.; Xu, J.; Butterfield, Z.; Chand, D.; Dubey, M. K.; Pekour, M. S.; Springston, S.; Zhang, Q. Regional Influence of Aerosol Emissions from Wildfires Driven by Combustion Efficiency: Insights from the BBOP Campaign. *Environ. Sci. Technol.* **2016**, *50* (16), 8613–8622.
(18) Sekimoto, K.; Koss, A. R.; Gilman, J. B.; Selimovic, V.; Coggon, M. M.; Zarzana, K. J.; Yuan, B.; Lerner, B. M.; Brown, S. S.; Warneke, C.; Yokelson, R. J.; Roberts, J. M.; de Gouw, J. High- and Low-Temperature Pyrolysis Profiles Describe Volatile Organic Compound Emissions from Western US Wildfire Fuels. *Atmos. Chem. Phys.* **2018**, *18* (13), 9263–9281.
(19) Roberts, J. M.; Stockwell, C. E.; Yokelson, R. J.; de Gouw, J.; Liu, Y.; Selimovic, V.; Koss, A. R.; Sekimoto, K.; Coggon, M. M.; Yuan, B.; Zarzana, K. J.; Brown, S. S.; Santin, C.; Doerr, S. H.; Warneke, C. The Nitrogen Budget of Laboratory-Simulated Western US Wildfires during the FIREX 2016 Fire Lab Study, 2020. https://doi.org/10.5194/acp-20-8807-2020.
(20) Hodshire, A. L.; Akherati, A.; Alvarado, M. J.; Brown-Steiner, B.; Jathar, S. H.; Jimenez, J. L.; Kreidenweis, S. M.; Lonsdale, C. R.; Onasch, T. B.; Ortega, A. M.; Pierce, J. R. Aging Effects on Biomass Burning Aerosol Mass and Composition: A Critical Review of Field and Laboratory Studies. *Environ. Sci. Technol.* **2019**, *53* (17), 10007–10022.
(21) May, A. A.; Levin, E. J. T.; Hennigan, C. J.; Riipinen, I.; Lee, T.; Collett, J. L., Jr.; Jimenez, J. L.; Kreidenweis, S. M.; Robinson, A. L. Gas-Particle Partitioning of Primary Organic Aerosol Emissions: 3. Biomass Burning. *J. Geophys. Res. D: Atmos.* **2013**, *118* (19), 11,327–11,338.
(22) Cubison, M. J.; Ortega, A. M.; Hayes, P. L.; Farmer, D. K.; Day, D.; Lechner, M. J.; Brune, W. H.; Apel, E.; Diskin, G. S.; Fisher, J. A.; Fuelberg, H. E.; Hecobian, A.; Knapp, D. J.; Mikoviny, T.; Riemer, D.; Sachse, G. W.; Sessions, W.; Weber, R. J.; Weinheimer, A. J.; Wisthaler, A.; Jimenez, J. L. Effects of Aging on Organic Aerosol from Open Biomass Burning Smoke in Aircraft and Laboratory Studies. *Atmos. Chem. Phys.* **2011**, *11* (23), 12049–12064.
(23) Hatch, L. E.; Yokelson, R. J.; Stockwell, C. E.; Veres, P. R.; Simpson, I. J.; Blake, D. R.; Orlando, J. J.; Barsanti, K. C. Multi-Instrument Comparison and Compilation of Non-Methane Organic Gas Emissions from Biomass Burning and Implications for Smoke-Derived Secondary Organic Aerosol Precursors. *Atmos. Chem. Phys.* **2017**, *17* (2), 1471–1489.
(24) Liu, X.; Huey, L. G.; Yokelson, R. J.; Selimovic, V.; Simpson, I. J.; Müller, M.; Jimenez, J. L.; Campuzano-Jost, P.; Beyersdorf, A. J.; Blake, D. R.; Butterfield, Z.; Choi, Y.; Crounse, J. D.; Day,

D. A.; Diskin, G. S.; Dubey, M. K.; Fortner, E.; Hanisco, T. F.; Hu, W.; King, L. E.; Kleinman, L.; Meinardi, S.; Mikoviny, T.; Onasch, T. B.; Palm, B. B.; Peischl, J.; Pollack, I. B.; Ryerson, T. B.; Sachse, G. W.; Sedlacek, A. J.; Shilling, J. E.; Springston, S.; St. Clair, J. M.; Tanner, D. J.; Teng, A. P.; Wennberg, P. O.; Wisthaler, A.; Wolfe, G. M. Airborne Measurements of Western U.S. Wildfire Emissions: Comparison with Prescribed Burning and Air Quality Implications. *J. Geophys. Res. D: Atmos.* **2017**, *122* (11), 6108–6129.

(25) Liu, X.; Zhang, Y.; Huey, L. G.; Yokelson, R. J.; Wang, Y.; Jimenez, J. L.; Campuzano-Jost, P.; Beyersdorf, A. J.; Blake, D. R.; Choi, Y.; St. Clair, J. M.; Crounse, J. D.; Day, D. A.; Diskin, G. S.; Ried, A.; Hall, S. R.; Hanisco, T. F.; King, L. E.; Meinardi, S.; Mikoviny, T.; Palm, B. B.; Peischl, J.; Perring, A. E.; Pollack, I. B.; Ryerson, T. B.; Sachse, G.; Schwarz, J. P.; Simpson, I. J.; Tanner, D. J.; Thornhil, K. L.; Ullmann, K.; Weber, R. J.; Wennberg, P. O.; Wisthaler, A.; Wolfe, G. M.; Ziemba, L. D. Agricultural Fires in the Southeastern U.S. during SEAC4RS: Emissions of Trace Gases and Particles and Evolution of Ozone, Reactive Nitrogen, and Organic Aerosol. *J. Geophys. Res.* **2016**, *121* (12), 7383–7414.

(26) May, A. A.; McMeeking, G. R.; Lee, T.; Taylor, J. W.; Craven, J. S.; Burling, I.; Sullivan, A. P.; Akagi, S.; Collett, J. L., Jr.; Flynn, M.; Coe, H.; Urbanski, S. P.; Seinfeld, J. H.; Yokelson, R. J.; Kreidenweis, S. M. Aerosol Emissions from Prescribed Fires in the United States: A Synthesis of Laboratory and Aircraft Measurements. *J. Geophys. Res. D: Atmos.* **2014**, *119* (20), 11,826–11,849.

(27) Wiggins, E. B.; Soja, A. J.; Gargulinski, E.; Halliday, H. S.; Pierce, R. B.; Schmidt, C. C.; Nowak, J. B.; DiGangi, J. P.; Diskin, G. S.; Katich, J. M.; Perring, A. E.; Schwarz, J. P.; Anderson, B. E.; Chen, G.; Crosbie, E. C.; Jordan, C.; Robinson, C. E.; Sanchez, K. J.; Shingler, T. J.; Shook, M.; Thornhill, K. L.; Winstead, E. L.; Ziemba, L. D.; Moore, R. H. High Temporal Resolution Satellite Observations of Fire Radiative Power Reveal Link between Fire Behavior and Aerosol and Gas Emissions. *Geophys. Res. Lett.* **2020**, *47* (23). https://doi.org/10.1029/2020gl090707.

(28) Wiggins, E. B.; Anderson, B. E.; Brown, M. D.; Campuzano-Jost, P.; Chen, G.; Crawford, J.; Crosbie, E. C.; Dibb, J.; DiGangi, J. P.; Diskin, G. S.; Fenn, M.; Gallo, F.; Gargulinski, E. M.; Guo, H.; Hair, J. W.; Halliday, H. S.; Ichoku, C.; Jimenez, J. L.; Jordan, C. E.; Katich, J. M.; Nowak, J. B.; Perring, A. E.; Robinson, C. E.; Sanchez, K. J.; Schueneman, M.; Schwarz, J. P.; Shingler, T. J.; Shook, M. A.; Soja, A. J.; Stockwell, C. E.; Thornhill, K. L.; Travis, K. R.; Warneke, C.; Winstead, E. L.; Ziemba, L. D.; Moore, R. H. Reconciling Assumptions in Bottom-up and Top-down Approaches for Estimating Aerosol Emission Rates from Wildland Fires Using Observations from FIREX-AQ. *J. Geophys. Res.* **2021**, *126* (24). https://doi.org/10.1029/2021jd035692.

(29) Palm, B. B.; Peng, Q.; Fredrickson, C. D.; Lee, B. H.; Garofalo, L. A.; Pothier, M. A.; Kreidenweis, S. M.; Farmer, D. K.; Pokhrel, R. P.; Shen, Y.; Murphy, S. M.; Permar, W.; Hu, L.; Campos, T. L.; Hall, S. R.; Ullmann, K.; Zhang, X.; Flocke, F.; Fischer, E. V.; Thornton, J. A. Quantification of Organic Aerosol and Brown Carbon Evolution in Fresh Wildfire Plumes. *Proc. Natl. Acad. Sci. U. S. A.* **2020**. https://doi.org/10.1073/pnas.2012218117.

(30) Pankow, J. F. An Absorption Model of Gas/particle Partitioning of Organic Compounds in the Atmosphere. *Atmos. Environ.* **1994**, *28* (2), 185–188.

(31) Donahue, N. M.; Robinson, A. L.; Stanier, C. O.; Pandis, S. N. Coupled Partitioning, Dilution, and Chemical Aging of Semivolatile Organics. *Environ. Sci. Technol.* **2006**, *40* (8), 2635–2643.

(32) Hodshire, A. L.; Bian, Q.; Ramnarine, E.; Lonsdale, C. R.; Alvarado, M. J.; Kreidenweis, S. M.; Jathar, S. H.; Pierce, J. R. More Than Emissions and Chemistry: Fire Size, Dilution, and Background Aerosol Also Greatly Influence Near-Field Biomass Burning Aerosol Aging. *J. Geophys. Res. D: Atmos.* **2019**, *124* (10), 5589–5611.

(33) Clarke, A. D. A Thermo-Optic Technique for in Situ Analysis of Size-Resolved Aerosol Physicochemistry. *Atmospheric Environment. Part A. General Topics* **1991**, *25* (3), 635–644.

(34) Ye, X.; Arab, P.; Ahmadov, R.; James, E.; Grell, G. A.; Pierce, B.; Kumar, A.; Makar, P.; Chen, J.; Davignon, D.; Carmichael, G. R.; Ferrada, G.; McQueen, J.; Huang, J.; Kumar, R.; Emmons, L.; Herron-Thorpe, F. L.; Parrington, M.; Engelen, R.; Peuch, V.-H.; da Silva, A.; Soja, A.; Gargulinski, E.; Wiggins, E.; Hair, J. W.; Fenn, M.; Shingler, T.; Kondragunta, S.; Lyapustin, A.; Wang, Y.;

Holben, B.; Giles, D. M.; Saide, P. E. Evaluation and Intercomparison of Wildfire Smoke Forecasts from Multiple Modeling Systems for the 2019 Williams Flats Fire. *Atmos. Chem. Phys.* **2021**, *21* (18), 14427–14469.

(35) Warneke, C.; Schwarz, J. P.; Dibb, J.; Kalashnikova, O.; Frost, G.; Al-Saad, J.; Brown, S. S.; Brewer, W. A.; Soja, A.; Seidel, F. C.; Washenfelder, R. A.; Wiggins, E. B.; Moore, R. H.; Anderson, B. E.; Jordan, C.; Yacovitch, T. I.; Herndon, S. C.; Liu, S.; Kuwayama, T.; Jaffe, D.; Johnston, N.; Selimovic, V.; Yokelson, R.; Giles, D. M.; Holben, B. N.; Goloub, P.; Popovici, I.; Trainer, M.; Kumar, A.; Pierce, R. B.; Fahey, D.; Roberts, J.; Gargulinski, E. M.; Peterson, D. A.; Ye, X.; Thapa, L. H.; Saide, P. E.; Fite, C. H.; Holmes, C. D.; Wang, S.; Coggon, M. M.; Decker, Z. C. J.; Stockwell, C. E.; Xu, L.; Gkatzelis, G.; Aikin, K.; Lefer, B.; Kaspari, J.; Griffin, D.; Zeng, L.; Weber, R.; Hastings, M.; Chai, J.; Wolfe, G. M.; Hanisco, T. F.; Liao, J.; Campuzano Jost, P.; Guo, H.; Jimenez, J. L.; Crawford, J.; The FIREX-AQ Science Team. Fire Influence on Regional to Global Environments and Air Quality (FIREX-AQ). *J. Geophys. Res.* **2023**, *128* (2). https://doi.org/10.1029/2022jd037758.

(36) Pagonis, D.; Campuzano-Jost, P.; Guo, H.; Day, D. A.; Schueneman, M. K.; Brown, W. L.; Nault, B. A.; Stark, H.; Siemens, K.; Laskin, A.; Piel, F.; Tomsche, L.; Wisthaler, A.; Coggon, M. M.; Gkatzelis, G. I.; Halliday, H. S.; Krechmer, J. E.; Moore, R. H.; Thomson, D. S.; Warneke, C.; Wiggins, E. B.; Jimenez, J. L. Airborne Extractive Electrospray Mass Spectrometry Measurements of the Chemical Composition of Organic Aerosol. *Atmospheric Measurement Techniques* **2021**, *14* (2), 1545–1559.

(37) Garofalo, L. A.; Pothier, M. A.; Levin, E. J. T.; Campos, T.; Kreidenweis, S. M.; Farmer, D. K. Emission and Evolution of Submicron Organic Aerosol in Smoke from Wildfires in the Western United States. *ACS Earth and Space Chemistry* **2019**, *3*, 1237–1247.

(38) DeCarlo, P. F.; Kimmel, J. R.; Trimborn, A.; Northway, M. J.; Jayne, J. T.; Aiken, A. C.; Gonin, M.; Fuhrer, K.; Horvath, T.; Docherty, K. S.; Worsnop, D. R.; Jimenez, J. L. Field-Deployable, High-Resolution, Time-of-Flight Aerosol Mass Spectrometer. *Anal. Chem.* **2006**, *78* (24), 8281–8289.

(39) Lopez-Hilfiker, F. D.; Pospisilova, V.; Huang, W.; Kalberer, M.; Mohr, C.; Stefenelli, G.; Thornton, J. A.; Baltensperger, U.; Prevot, A. S. H.; Slowik, J. G. An Extractive Electrospray Ionization Time-of-Flight Mass Spectrometer (EESI-TOF) for Online Measurement of Atmospheric Aerosol Particles. *Atmos. Meas. Tech.* **2019**, *12* (9), 4867–4886.

(40) Onasch, T. B.; Trimborn, A.; Fortner, E. C.; Jayne, J. T.; Kok, G. L.; Williams, L. R.; Davidovits, P.; Worsnop, D. R. Soot Particle Aerosol Mass Spectrometer: Development, Validation, and Initial Application. *Aerosol Sci. Technol.* **2012**, *46* (7), 804–817.

(41) Kang, E.; Root, M. J.; Toohey, D. W.; Brune, W. H. Introducing the Concept of Potential Aerosol Mass (PAM). *Atmos. Chem. Phys.* **2007**, *7* (22), 5727–5744.

(42) Ortega, A. M.; Hayes, P. L.; Peng, Z.; Palm, B. B.; Hu, W.; Day, D. A.; Li, R.; Cubison, M. J.; Brune, W. H.; Graus, M.; Warneke, C.; Gilman, J. B.; Kuster, W. C.; de Gouw, J.; Gutiérrez-Montes, C.; Jimenez, J. L. Real-Time Measurements of Secondary Organic Aerosol Formation and Aging from Ambient Air in an Oxidation Flow Reactor in the Los Angeles Area. *Atmos. Chem. Phys.* **2016**, *16* (11), 7411–7433.

(43) Nault, B. A.; Campuzano-Jost, P.; Day, D. A.; Schroder, J. C.; Anderson, B.; Beyersdorf, A. J.; Blake, D. R.; Brune, W. H.; Choi, Y.; Corr, C. A.; de Gouw, J. A.; Dibb, J.; DiGangi, J. P.; Diskin, G. S.; Fried, A.; Huey, L. G.; Kim, M. J.; Knote, C. J.; Lamb, K. D.; Lee, T.; Park, T.; Pusede, S. E.; Scheuer, E.; Thornhill, K. L.; Woo, J.-H.; Jimenez, J. L. Secondary Organic Aerosol Production from Local Emissions Dominates the Organic Aerosol Budget over Seoul, South Korea, during KORUS-AQ. *Atmos. Chem. Phys.* **2018**, *18* (24), 17769–17800.

(44) Heim, E. W.; Dibb, J.; Scheuer, E.; Jost, P. C.; Nault, B. A.; Jimenez, J. L.; Peterson, D.; Knote, C.; Fenn, M.; Hair, J.; Beyersdorf, A. J.; Corr, C.; Anderson, B. E. Asian Dust Observed during KORUS-AQ Facilitates the Uptake and Incorporation of Soluble Pollutants during Transport to South Korea. *Atmos. Environ.* **2020**, *224*, 117305.

(45) Guo, H.; Campuzano-Jost, P.; Nault, B. A.; Day, D. A.; Schroder, J. C.; Kim, D.; Dibb, J. E.;

Dollner, M.; Weinzierl, B.; Jimenez, J. L. The Importance of Size Ranges in Aerosol Instrument Intercomparisons: A Case Study for the Atmospheric Tomography Mission. *Atmos. Meas. Tech.* **2021**, *14* (5), 3631–3655.
(46) Brown, W. L.; Day, D. A.; Stark, H.; Pagonis, D.; Krechmer, J. E.; Liu, X.; Price, D. J.; Katz, E. F.; DeCarlo, P. F.; Masoud, C. G.; Wang, D. S.; Hildebrandt Ruiz, L.; Arata, C.; Lunderberg, D. M.; Goldstein, A. H.; Farmer, D. K.; Vance, M. E.; Jimenez, J. L. Real-Time Organic Aerosol Chemical Speciation in the Indoor Environment Using Extractive Electrospray Ionization Mass Spectrometry. *Indoor Air* **2020**, *31* (1), 141–155.
(47) Ward, D. E.; Radke, L. F. Emissions Measurements From Vegetation Fires: A Comparative Evaluation of Methods and Results. In *Fire in the Environment: The Ecological, Atmospheric and Climatic Importance of Vegetation Fires*; J, C. P., Goldammer, J. G., Eds.; John Wiley: New York, 1993; pp 53–76.
(48) Susott, R. A.; Olbu, G. J.; Baker, S. P.; Ward, D. E.; Kauffman, J. B.; Shea, R. Carbon, Hydrogen, Nitrogen, and Thermo-Gravimetric Analysis of Tropical Ecosystem Biomass. In *Biomass Burning and Global Change*; Levine, J. S., Ed.; MIT Press: Cambridge, MA, 1996; pp 350–360.
(49) Stockwell, C. E.; Yokelson, R. J.; Kreidenweis, S. M.; Robinson, A. L.; DeMott, P. J.; Sullivan, R. C.; Reardon, J.; Ryan, K. C.; Griffith, D. W. T.; and Stevens, L. Trace gas emissions from combustion of peat, crop residue, domestic biofuels, grasses, and other fuels: configuration and Fourier transform infrared (FTIR) component of the fourth Fire Lab at Missoula Experiment (FLAME-4). *Atmos. Chem. Phys.* **2014**, *14*, 9727-9754.
(50) NOAA. NOWData - NOAA Online Weather Data, 2021. https://www.weather.gov/wrh/climate?wfo=mso (accessed 2021).
(51) Cappa, C. D. A Model of Aerosol Evaporation Kinetics in a Thermodenuder. *Atmos. Meas. Tech.* **2010**, *3* (3), 579–592.
(52) Shingler, T.; Crosbie, E.; Ortega, A.; Shiraiwa, M.; Zuend, A.; Beyersdorf, A.; Ziemba, L.; Anderson, B.; Thornhill, L.; Perring, A. E.; Schwarz, J. P.; Campazano-Jost, P.; Day, D. A.; Jimenez, J. L.; Hair, J. W.; Mikoviny, T.; Wisthaler, A.; Sorooshian, A. Airborne Characterization of Subsaturated Aerosol Hygroscopicity and Dry Refractive Index from the Surface to 6.5 Km during the SEAC 4 RS Campaign : DASH-SP Measurements in SEAC 4 RS. *J. Geophys. Res. D: Atmos.* **2016**, *121* (8), 4188–4210.
(53) Theodoritsi, G. N.; Ciarelli, G.; Pandis, S. N. Simulation of the Evolution of Biomass Burning Organic Aerosol with Different Volatility Basis Set Schemes in PMCAMx-SRv1.0. *Geoscientific Model Development*. 2021, pp 2041–2055. https://doi.org/10.5194/gmd-14-2041-2021.
(54) Hatch, L. E.; Rivas-Ubach, A.; Jen, C. N.; Lipton, M.; Goldstein, A. H.; Barsanti, K. C. Measurements of I/SVOCs in Biomass-Burning Smoke Using Solid-Phase Extraction Disks and Two-Dimensional Gas Chromatography. *Atmos. Chem. Phys.* **2018**, *18* (24), 17801–17817.
(55) Cappa, C. D.; Jimenez, J. L. Quantitative Estimates of the Volatility of Ambient Organic Aerosol. *Atmos. Chem. Phys.* **2010**, *10* (12), 5409–5424.
(56) May, A. A.; Saleh, R.; Hennigan, C. J.; Donahue, N. M.; Robinson, A. L. Volatility of Organic Molecular Markers Used for Source Apportionment Analysis: Measurements and Implications for Atmospheric Lifetime. *Environmental Science and Technology* **2012**, *46* (22), 12435–12444.
(57) Fredrickson, C. D.; Palm, B. B.; Lee, B. H.; Zhang, X.; Orlando, J. J.; Tyndall, G. S.; Garofalo, L. A.; Pothier, M. A.; Farmer, D. K.; Decker, Z. C. J.; Robinson, M. A.; Brown, S. S.; Murphy, S. M.; Shen, Y.; Sullivan, A. P.; Schobesberger, S.; Thornton, J. A. Formation and Evolution of Catechol-Derived SOA Mass, Composition, Volatility, and Light Absorption. *ACS Earth Space Chem.* **2022**, *6* (4), 1067–1079.
(58) Finewax, Z.; De Gouw, J. A.; Ziemann, P. J. Identification and Quantification of 4-Nitrocatechol Formed from OH and NO3 Radical-Initiated Reactions of Catechol in Air in the Presence of NOx: Implications for Secondary Organic Aerosol Formation from Biomass Burning. *Environmental Science and Technology* **2018**, *52* (4), 1981–1989.
(59) Liu, X.; Day, D. A.; Krechmer, J. E.; Ziemann, P. J.; Jimenez, J. L. Determining Activity

Coefficients of SOA from Isothermal Evaporation in a Laboratory Chamber. *Environ. Sci. Technol. Lett.* **2021**, *8* (3), 212–217.
(60) Coggon, M. M.; Veres, P. R.; Yuan, B.; Koss, A.; Warneke, C.; Gilman, J. B.; Lerner, B. M.; Peischl, J.; Aikin, K. C.; Stockwell, C. E.; Hatch, L. E.; Ryerson, T. B.; Roberts, J. M.; Yokelson, R. J.; and de Gouw, J. A. Emissions of nitrogen-containing organic compounds from the burning of herbaceous and arboraceous biomass: Fuel composition dependence and the variability of commonly used nitrile tracers. *Geophys. Res. Lett.* **2016**, *43*, 9903-9912.
(61) Ahmadov, R.; James, E. *HRRR: The High-Resolution Rapid Refresh Smoke Modeling System*. https://rapidrefresh.noaa.gov/hrrr/HRRRsmoke/HRRR-Smoke_desc.html (accessed 2022-06-30).
(62) Emerson, E. W.; Hodshire, A. L.; DeBolt, H. M.; Bilsback, K. R.; Pierce, J. R.; McMeeking, G. R.; Farmer, D. K. Revisiting Particle Dry Deposition and Its Role in Radiative Effect Estimates. *Proc. Natl. Acad. Sci. U. S. A.* **2020**, *117* (42), 26076–26082.